Heavy Quarkonia Melting in QGP Using Deep Neural Networks

Machine-Learned Quarkonium Dissociation in Hot QCD Matter: A Unified Framework

Presenter: Mohammad Yousuf Jamal

Affiliation: Central China Normal University, Wuhan, China

華中師範大學
CENTRAL CHINA NORMAL UNIVERSITY

ML is helping in high-energy / heavy-ion / QGP physics research in different ways

- Learning QGP medium properties directly from lattice or theory data (screening masses, effective couplings, EoS)

  F.P. Li et al., Phys. Lett. B 844, 138088 (2023)

- Reconstructing in-medium spectral functions and complex potentials for quarkonia

  A. Kades et al., Phys. Rev. D 102, 096001 (2020)
  arXiv:2509.14970 [hep-ph]

- Acting as fast Emulators for expensive simulations and high-dimensional parameter scans

  L. G. Pang et al., Nature. Commun. 9, 210 (2018)

- Calibrating theory to experiment to extract QGP transport coefficients with quantified uncertainties

  J.E. Bernhard et al., Phys. Rev. C 94, 024907 (2016)

- Applications to jet quenching, heavy-quark diffusion, and event characterization

  (see e.g. recent ML studies in jet/QGP tomography literature)

Flow of the talk

1. Quarkonia in High-Energy Collisions

2. Dissociation in the QGP Medium

3. Machine Learning Approach to In-Medium Quarkonia

4. Future Directions

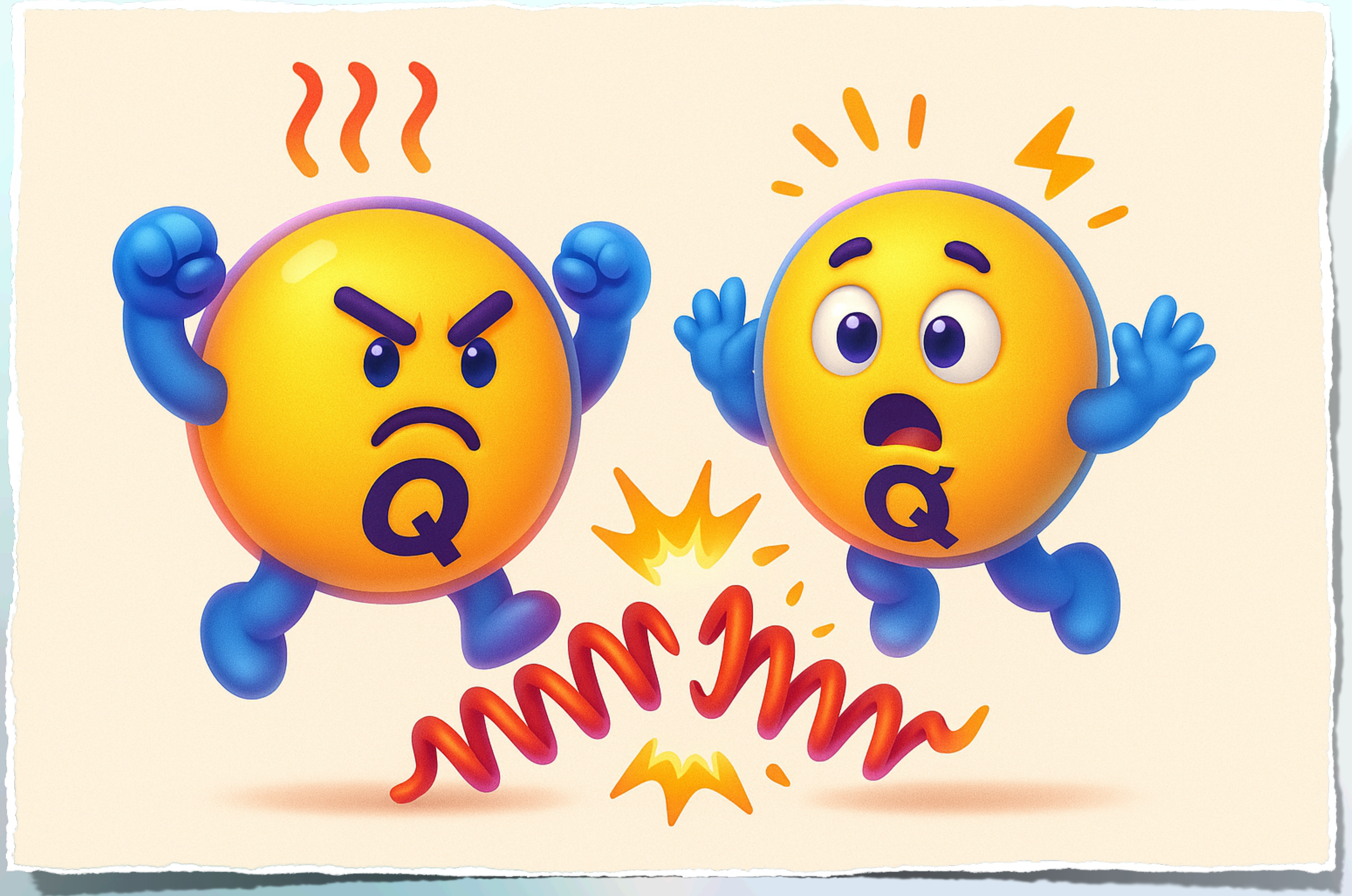

Based on: arXiv:2509.14970 [hep-ph]

Collaboration: Fu-Peng Li, Long-Gang Pang, and Guang-You Qin

Quarkonia in High-Energy Collisions

Heavy Quarkonia Production

- Heavy quark pairs created in initial hard scatterings ($\tau \lesssim 0.1$ fm/c)

- Formation time comparable to early QGP evolution

- Quarkonia propagate through evolving, anisotropic medium

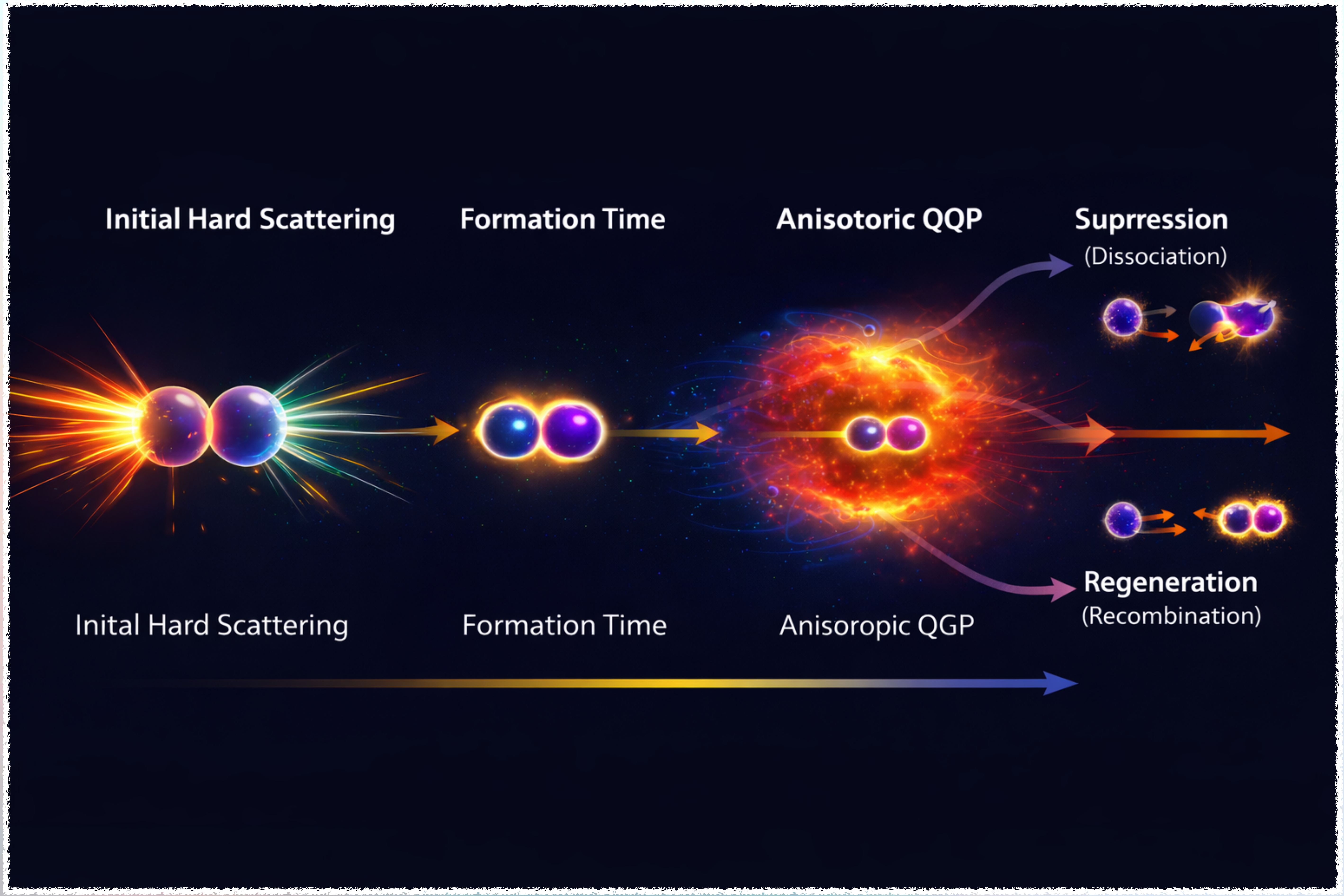

- Competing suppression and regeneration mechanisms

Heavy Quarkonia as Multiscale Systems

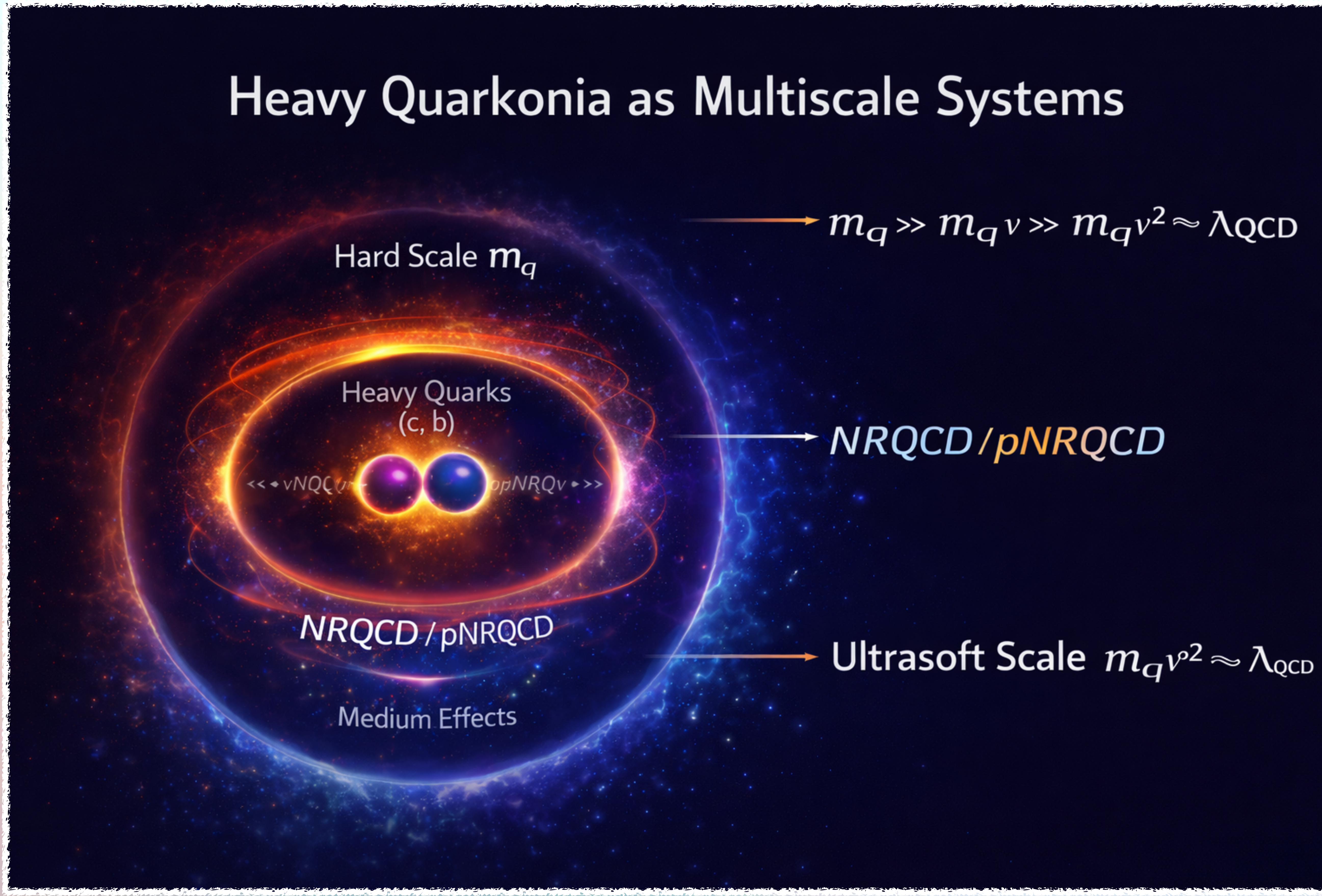

- Hierarchy: $(m_q \gg m_q v \gg m_q v^2 \sim \Lambda_{\mathrm{QCD}})$

- Separation of hard, soft, and ultrasoft scales

- Medium effects modify the potential at soft scales

- Nonrelativistic bound states described by NRQCD / pNRQCD

Spectroscopy and Binding Systematics

- Cornell-type potential captures short- and long-distance physics

- State hierarchy: tightly bound (1S) vs loosely bound excited states

- Radii and binding energies determine sensitivity to medium scales

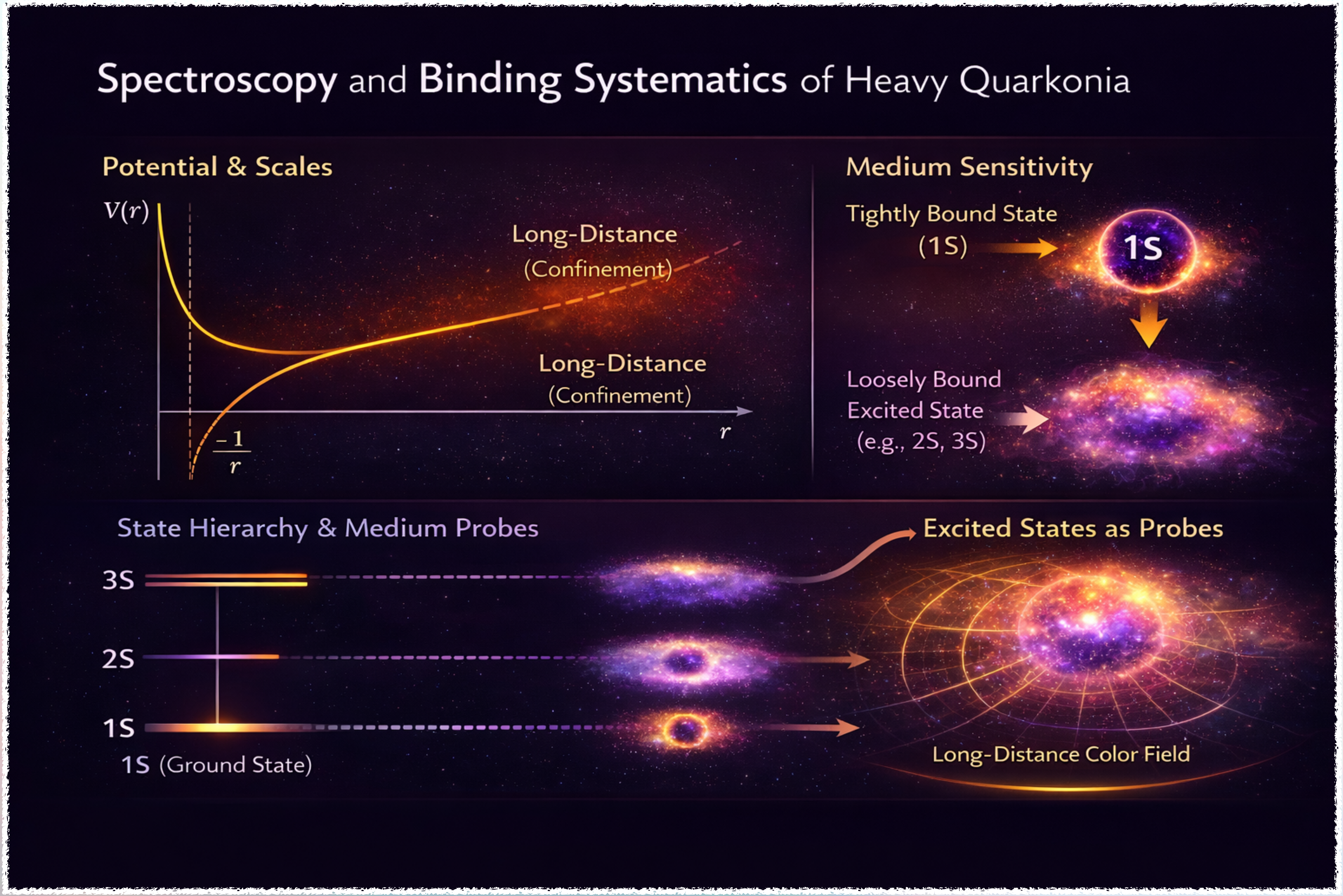

- Excited states probe longer-distance color fields

Sequential Suppression

- Dissociation occurs when screening length (r_D) ≲ quarkonium radius

- Larger, weakly bound states melt earlier

- Ground states survive deeper into QGP phase

- Provides a tomographic probe of medium screening scale

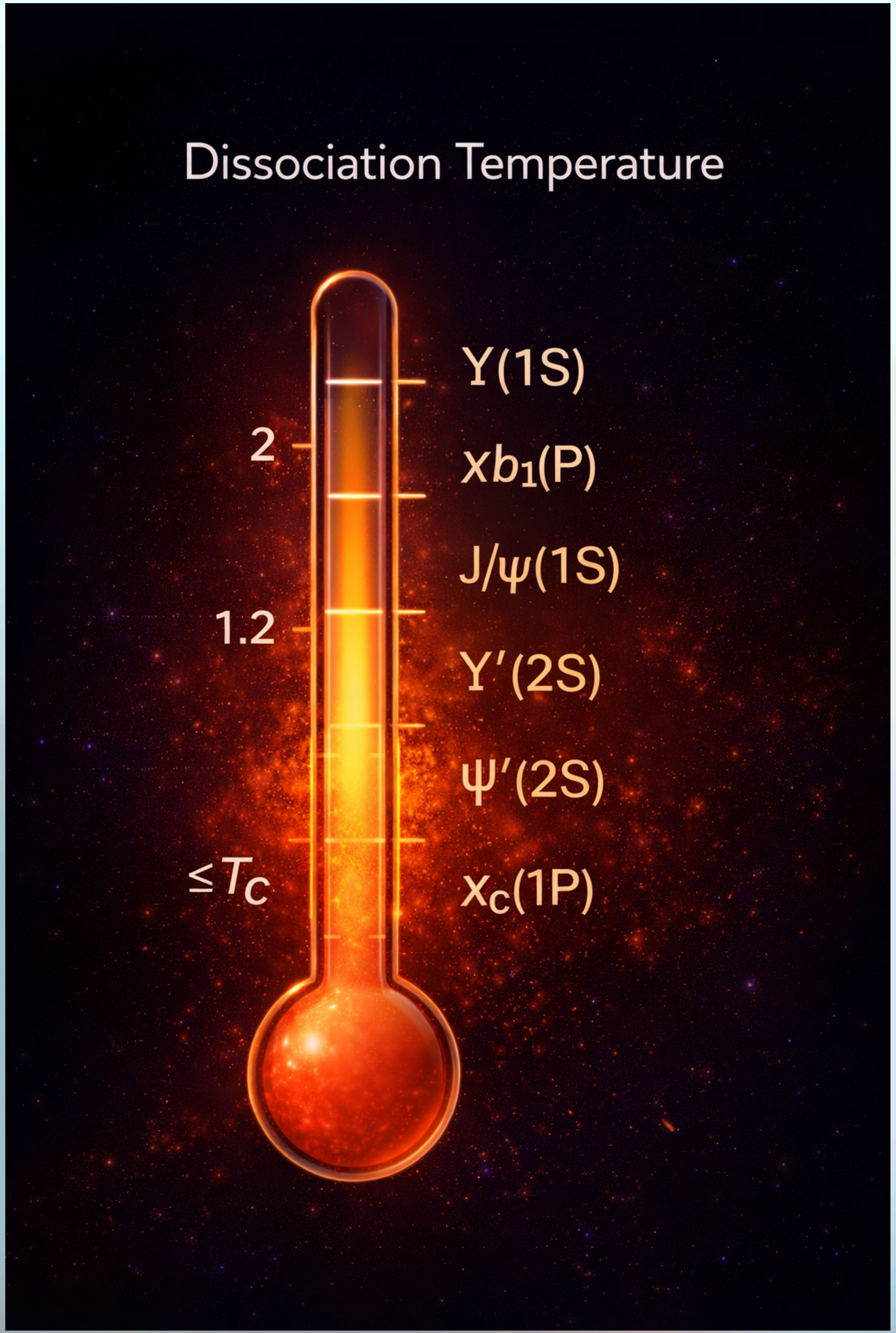

Why Quarkonia Remain Unique Probes

- Sensitive to both static screening and dynamical scattering
- Connects lattice QCD, effective theory, and heavy-ion phenomenology
- Complementary to jet quenching and bulk observables
- Ideal system for studying real-time QCD in a thermal medium

Dissociation in the QGP Medium

Process of Dissociation

1. Vacuum Binding:

In vacuum, quarkonium can be described by the Cornell potential:

$$V_{\text{vac}}(r) = -\frac{\alpha}{r} + \sigma r \,. \quad \text{where } \alpha \text{ is the strong coupling and } \sigma \text{ is the string part.}$$

2. Medium Effects:

In the QGP, color screening modifies the potential and enables dissociation in the deconfined medium.

3. Complex In-Medium Potential:

Real part: mediates binding

Imaginary part: induces thermal decay width

4. Dissociation Process:

The competition between the binding and dissociation determines the fate of quarkonium state.

Schrödinger Solver and Thermal Widths

- Radial bound states from

$$\left[-\frac{1}{2\mu}\frac{d^2}{dr^2} + \Re V(r,T)\right] u_n(r,T) = E_n(T)\, u_n(r,T), \quad \psi_n = u_n/r,\ \mu = \frac{m_Q}{2}$$

- Binding energy with thermal continuum:

$$E_B(T) = V_\infty(T) - E_n(T)$$

- Thermal width from Landau damping:

$$\Gamma_n(T) = \int_0^\infty d^3r\,|\psi_n(r,T)|^2\left[-\ \Im V(r,T)\right]$$

M.Y.Jamal, F.P.Li, L.G.Pang and G.Y.Qin, [arXiv:2509.14970 [hep-ph]

Machine Learning Approach to In-Medium Quarkonia

ML Description: Deep-Learning Quasi-Parton Model (DLQPM)

- We have employed, Physics Informed Neural Network (PINN)

- Inputs $\rightarrow$ Model: use lattice $s(T)$ and $\Delta(T)$

  fit a quasiparticle EOS with $m_g(T), m_{u/d}(T), m_s(T)$.

- Network: DLQPM maps $T/T_c \rightarrow \{m_g, m_{u/d}, m_s\}$ with smoothness

  HTL-consistent high-T behavior.

- Output $\rightarrow$ calibrated $m_g(T), m_{u/d}(T), m_s(T)$ (with uncertainty)

F.P.Li, H.L.Lu, L.G.Pang and G.Y.Qin, PLB 844, 138088(2023)

Method: PINN

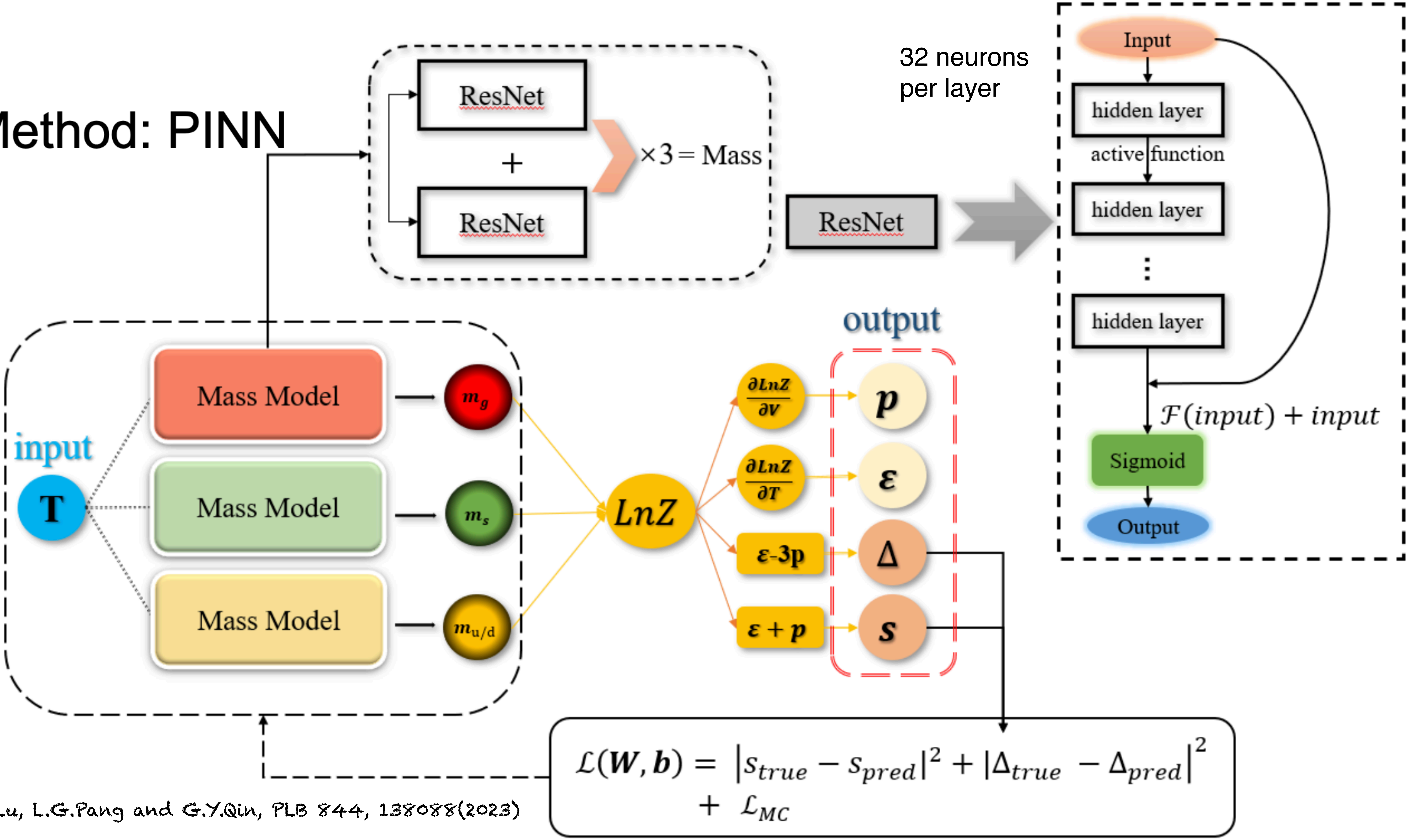

F.P.Li, H.L.Lu, L.G.Pang and G.Y.Qin, PLB 844, 138088(2023)

Method: PINN

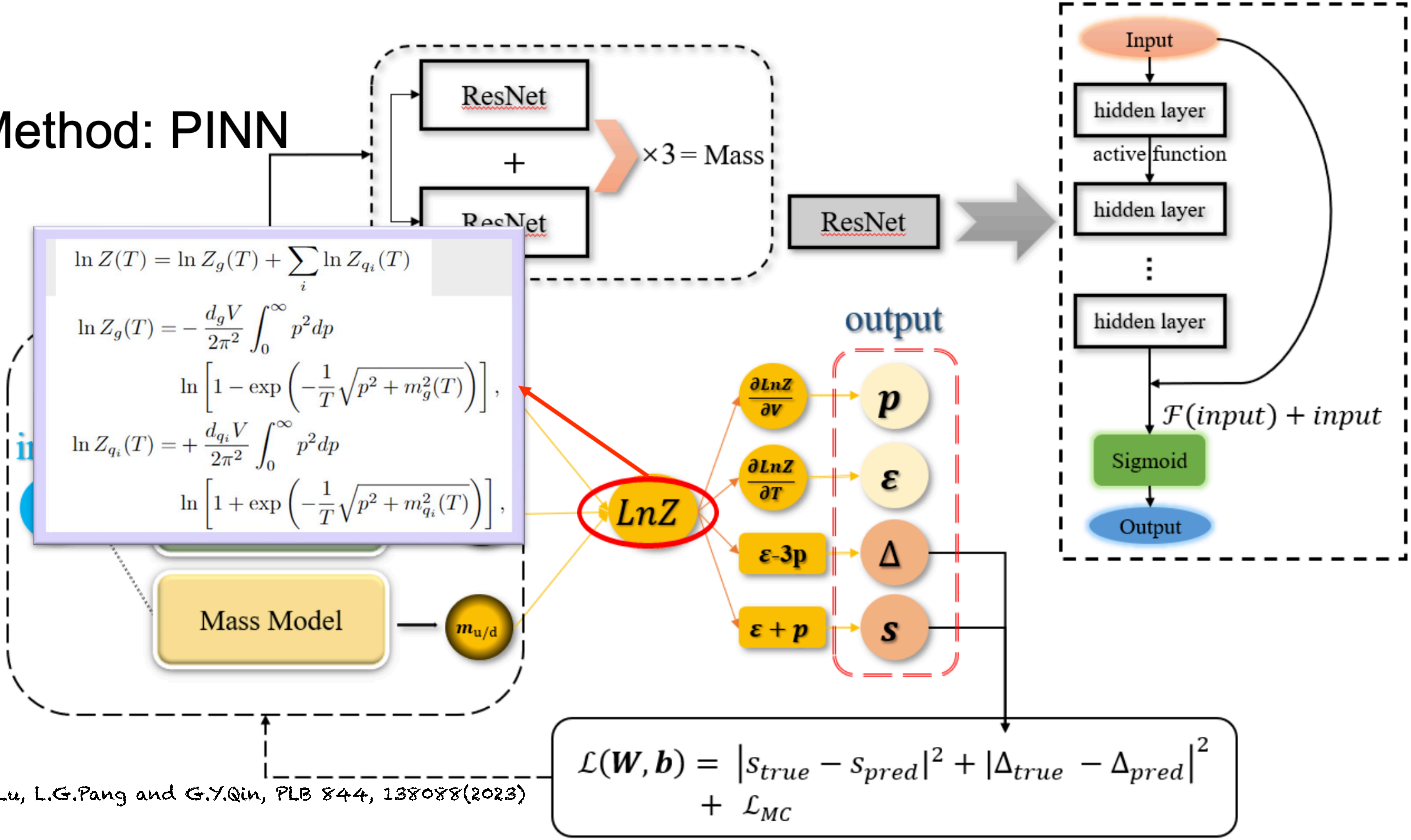

F.P.Li, H.L.Lu, L.G.Pang and G.Y.Qin, PLB 844, 138088(2023)

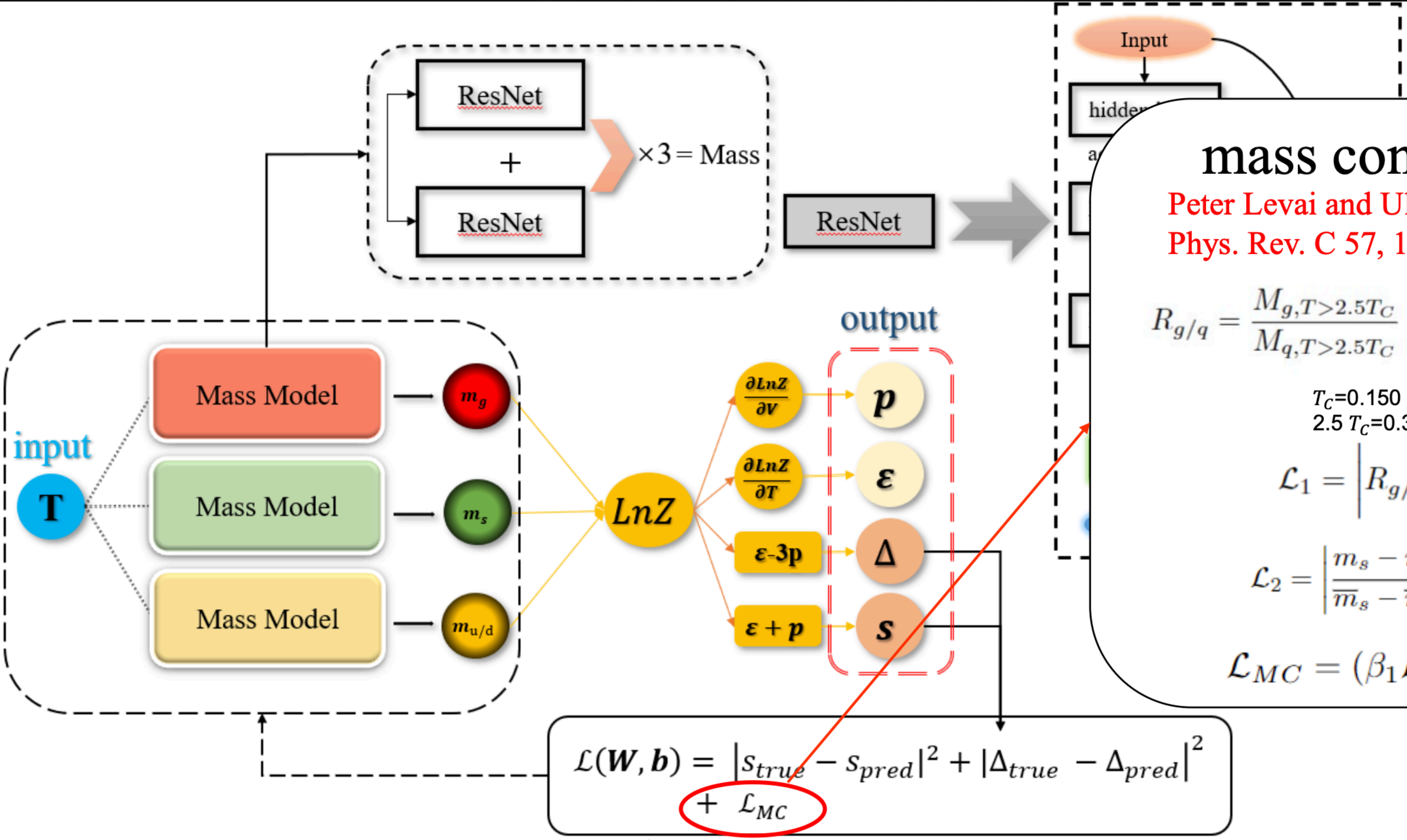

mass constraints

Peter Levai and Ulrich W. Heinz
Phys. Rev. C 57, 1879–1890 (1998

$$R_{g/q} = \frac{M_{g,T>2.5T_C}}{M_{q,T>2.5T_C}} = \sqrt{\frac{3}{2}\left(\frac{N_C}{3} + \frac{N_f}{6}\right)}$$

T_C=0.150 GeV
2.5 T_C=0.375GeV

$$\mathcal{L}_1 = \left| R_{g/q} - \frac{3}{2} \right| .$$

$$\mathcal{L}_2 = \left| \frac{m_s - m_{u/d}}{\overline{m}_s - \overline{m}_{u/d}} - 1 \right| .$$

$$\mathcal{L}_{MC} = (\beta_1 \mathcal{L}_1 + \beta_2 \mathcal{L}_2)^2$$

$$\mathcal{L}(\boldsymbol{W}, \boldsymbol{b}) = |s_{true} - s_{pred}|^2 + |\Delta_{true} - \Delta_{pred}|^2 + \mathcal{L}_{MC}$$

F.P.Li, H.L.Lu, L.G.Pang and G.Y.Qin, PLB 844, 138088(2023)

• Result: QCD EoS

After $50{,}000$ training epochs, the total error converges to approximately 10^{-5}

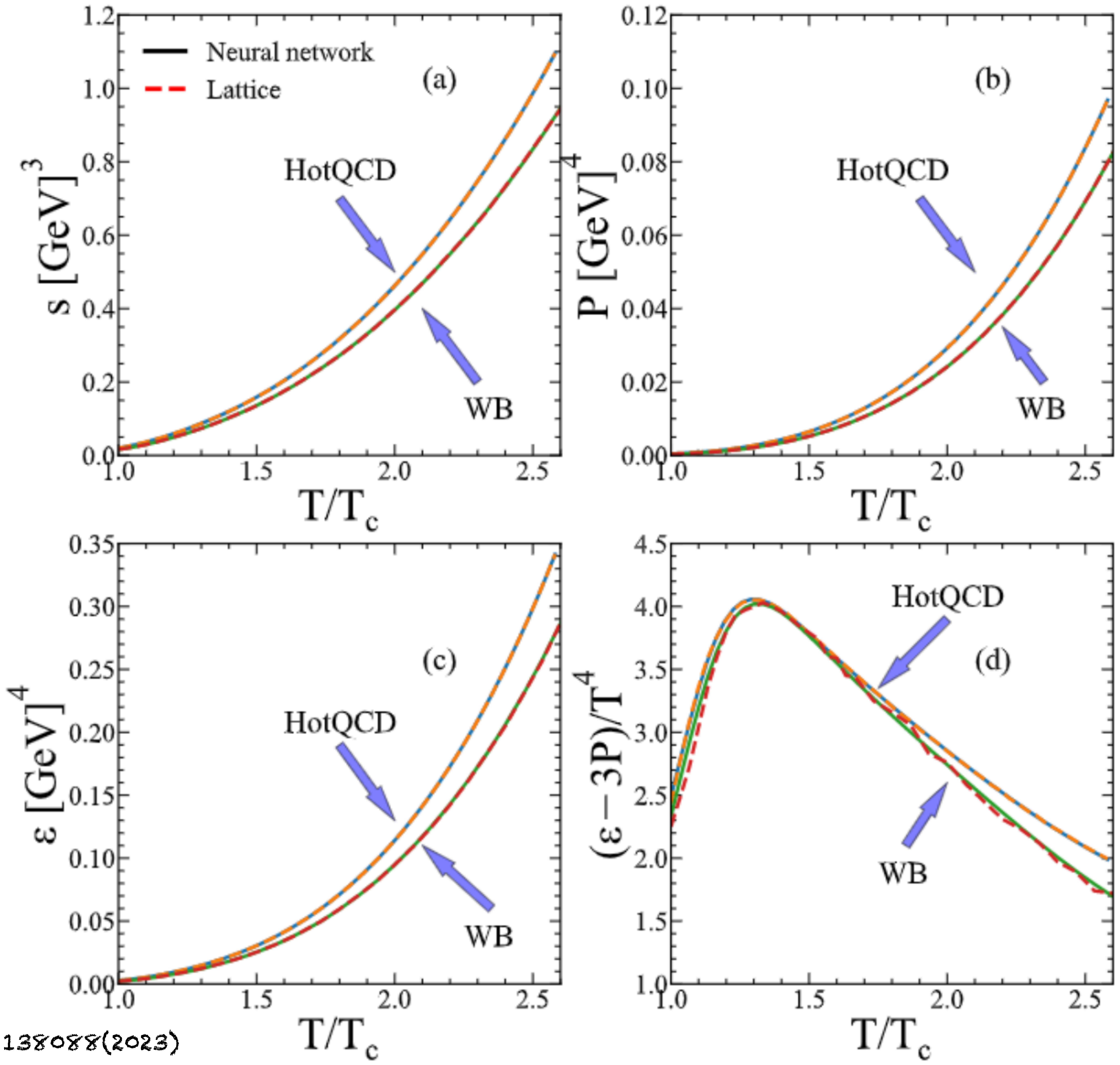

F.P.Li, H.L.Lu, L.G.Pang and G.Y.Qin, PLB 844, 138088(2023)

Outputs: $m_g(T), m_{u/d}(T)$ (from light–quark masses)

- Using DLQPM the masses are extracted
- Compared with other models

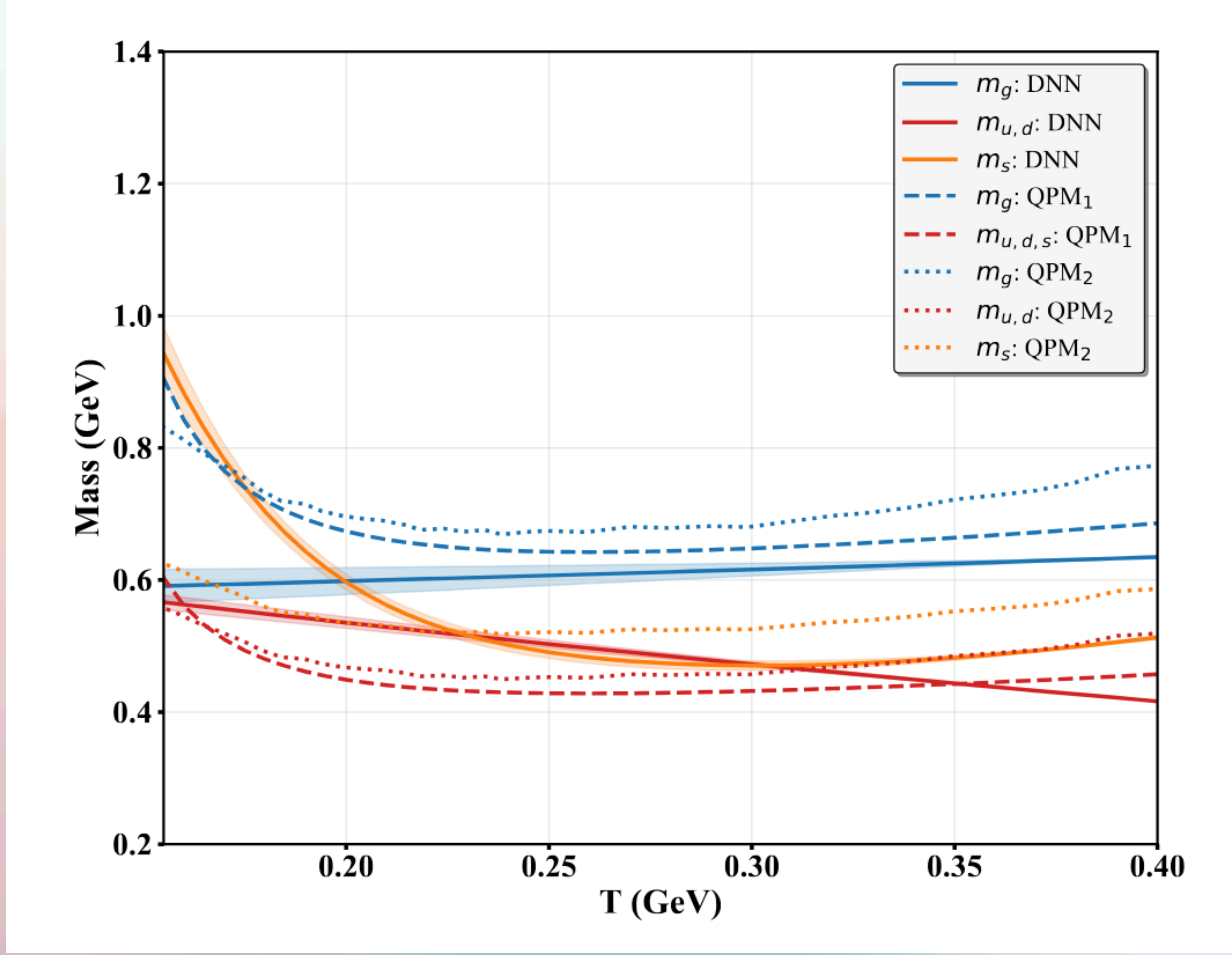

QPM 1: F.-L. Liu, W.-J. Xing, X.-Y. Wu, G.-Y. Qin, S. Cao,and X.-N. Wang, EPJC 82, 350 (2022)
QPM2: V. Mykhaylova, M. Bluhm, K. Redlich, and C. Sasaki, PRD 100, 034002 (2019)

HotQCD Collaboration (A. Bazavov et al.), PRD 90, 094503 (2014) — EOS training data.
M. Laine, O. Philipsen, P. Romatschke, M. Tassler, JHEP 03 (2007) 054 — HTL framework for screening.

Outputs: $g_s^2(T)$ (from light–quark masses)

- From DLQPM masses $\{m_g(T), m_{u/d}(T)\}$ extract $g_s(T)$:

$$m_g^2(T) = \frac{1}{6}\, g_s^2(T) \left(N_c + \tfrac{1}{2}N_f\right) T^2,\ m_{u/d}^2(T) = \frac{N_c^2 - 1}{8N_c}\, g_s^2(T)\, T^2,$$

$$\Rightarrow\ g_s^2(T) = \frac{m_g^2(T) + m_{u/d}^2(T)}{\frac{1}{6}\left(N_c + \frac{1}{2}N_f\right)T^2 + \frac{N_c^2 - 1}{8N_c}T^2}$$

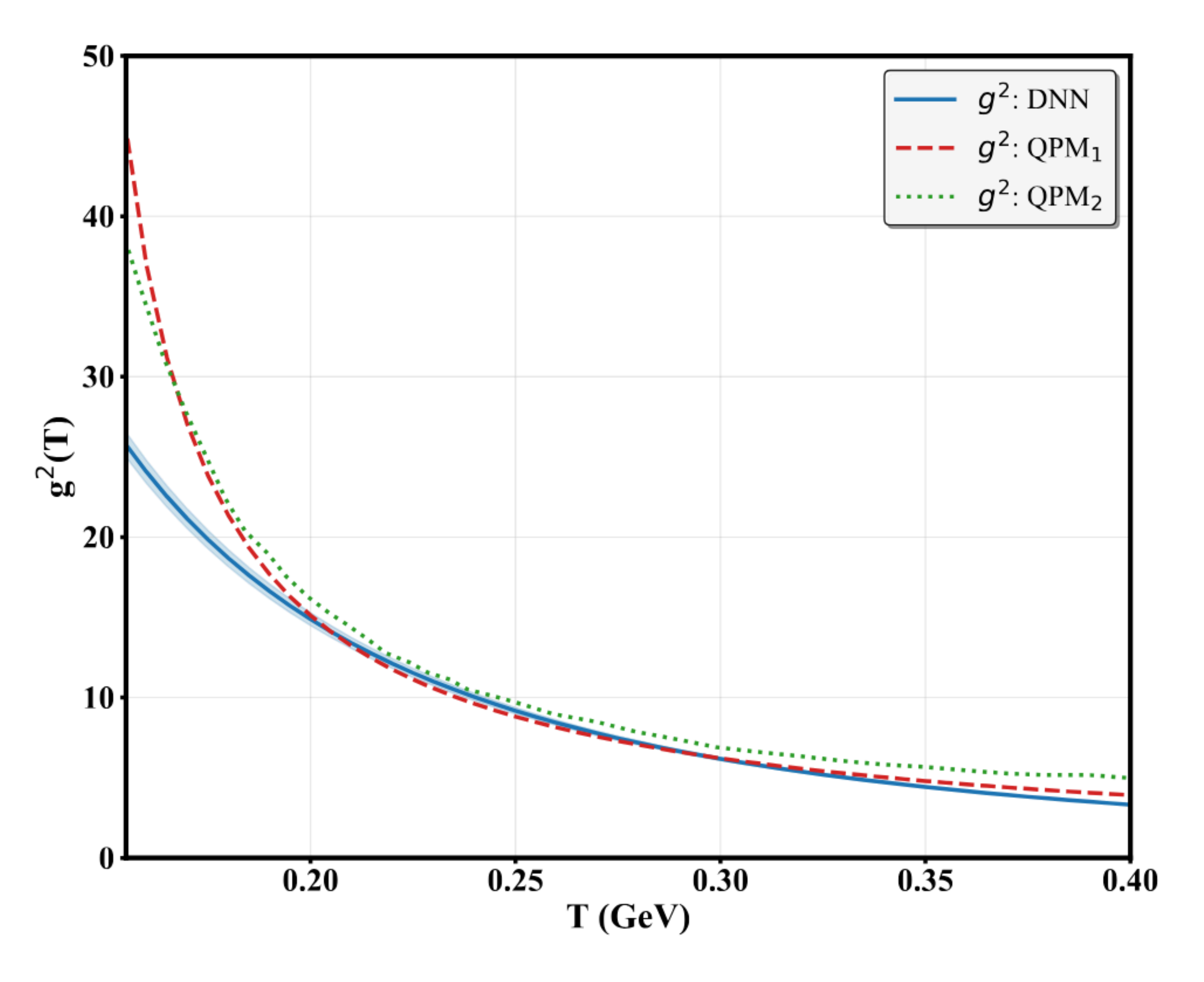

QPM 1: F.-L. Liu, W.-J. Xing, X.-Y. Wu, G.-Y. Qin, S. Cao,and X.-N. Wang, EPJC 82, 350 (2022)
QPM2: V. Mykhaylova, M. Bluhm, K. Redlich, and C. Sasaki, PRD 100, 034002 (2019)

HotQCD Collaboration (A. Bazavov et al.), Phys. Rev. D 90, 094503 (2014) — EOS training data.
M. Laine, O. Philipsen, P. Romatschke, M. Tassler, JHEP 03 (2007) 054 — HTL framework for screening.

Outputs: $m_D(T)$ (from light–quark masses)

- Debye mass from HTL:

$$m_D^2 = -\, g_s^2 \left(2N_c \int \frac{d^3q}{(2\pi)^3} \partial_q f_g(\mathbf{q}) + 2N_f \int \frac{d^3q}{(2\pi)^3} \partial_q f_q(\mathbf{q}) \right)$$

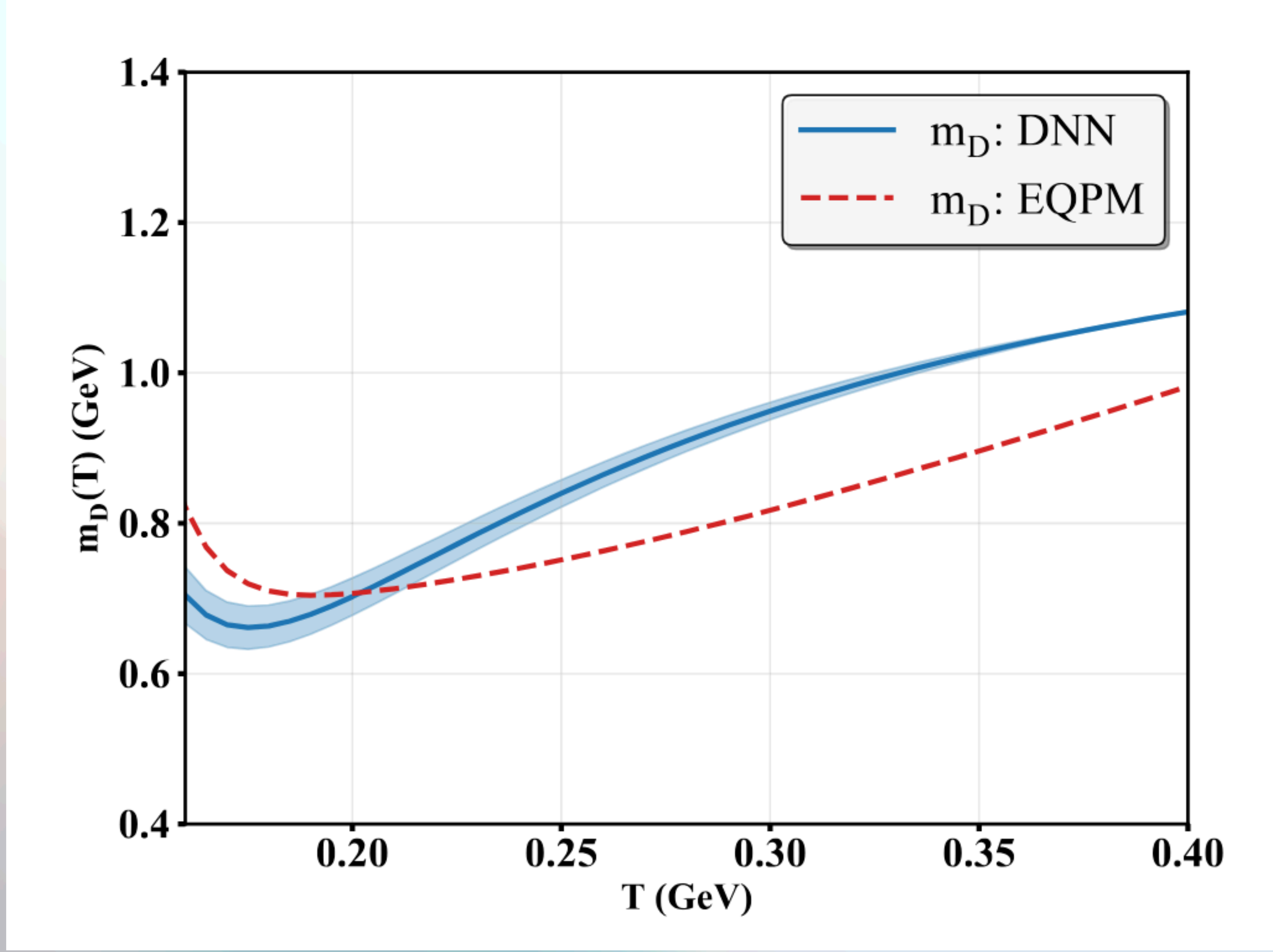

Where $f_{q,g}(\mathbf{q})$ are the medium particle distribution functions with finite thermal masses

HotQCD Collaboration (A. Bazavov et al.), Phys. Rev. D 90, 094503 (2014) — EOS training data.
M. Laine, O. Philipsen, P. Romatschke, M. Tassler, JHEP 03 (2007) 054 — HTL framework for screening.
EQPM: M. Y. Jamal, S. Mitra, and V. Chandra, Phys. Rev. D 95, 094022 (2017),

Complex In-Medium Potential: Real and Imaginary Parts

- Vacuum baseline: Cornell $V_{\text{vac}}(r) = -\alpha/r + \sigma r$.
- Medium Modification → Real and Imaginary Parts of Potential
- $\Re V(r = 0.5\,\text{fm}, T)$: becomes less attractive with T/T_c → screening weakens binding.
- $\Im V(r = 0.5\,\text{fm}, T)$: magnitude grows → in-medium damping
- Together: higher T means shallower well + stronger damping → quarkonium is easier to melt.

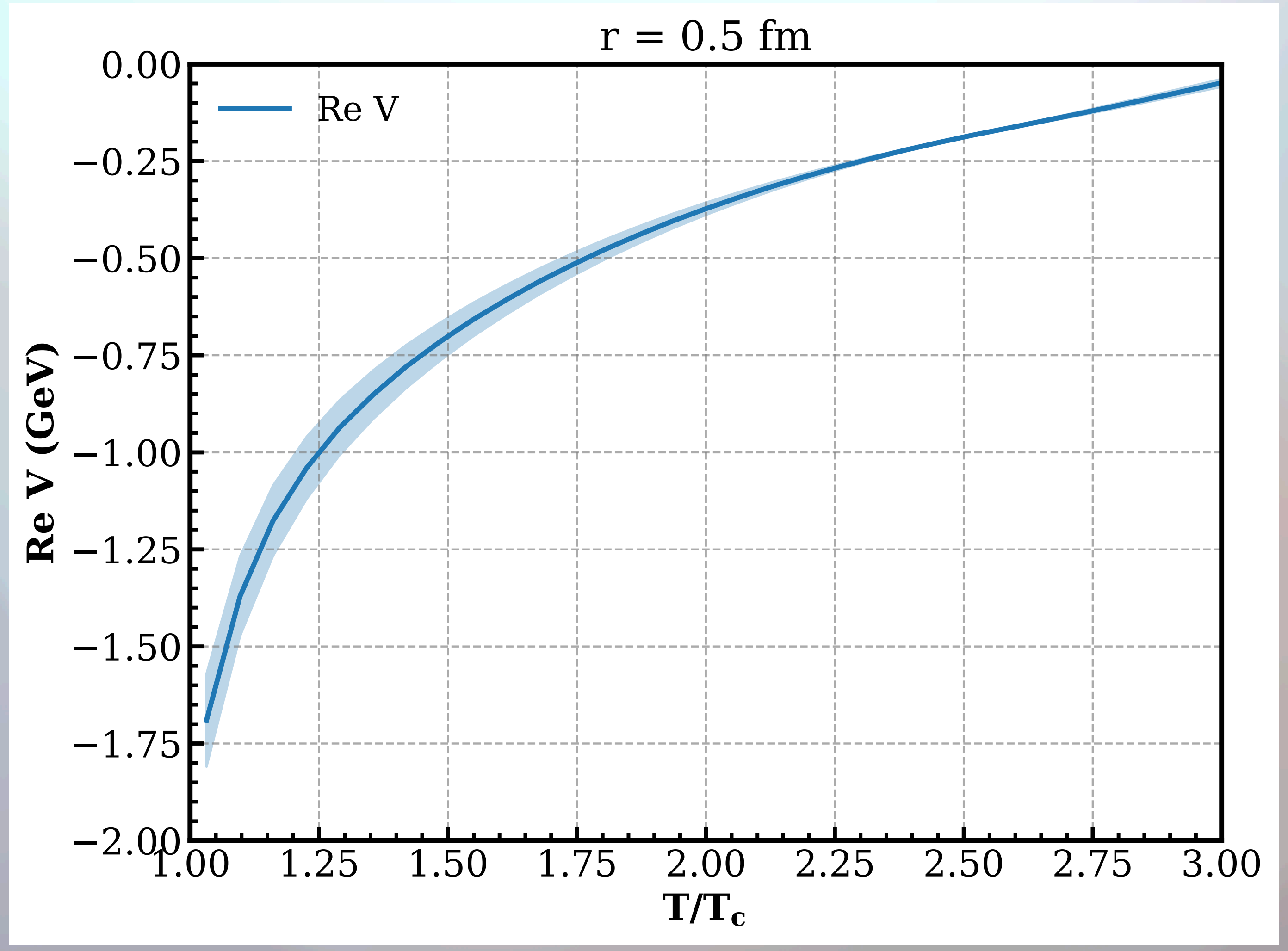

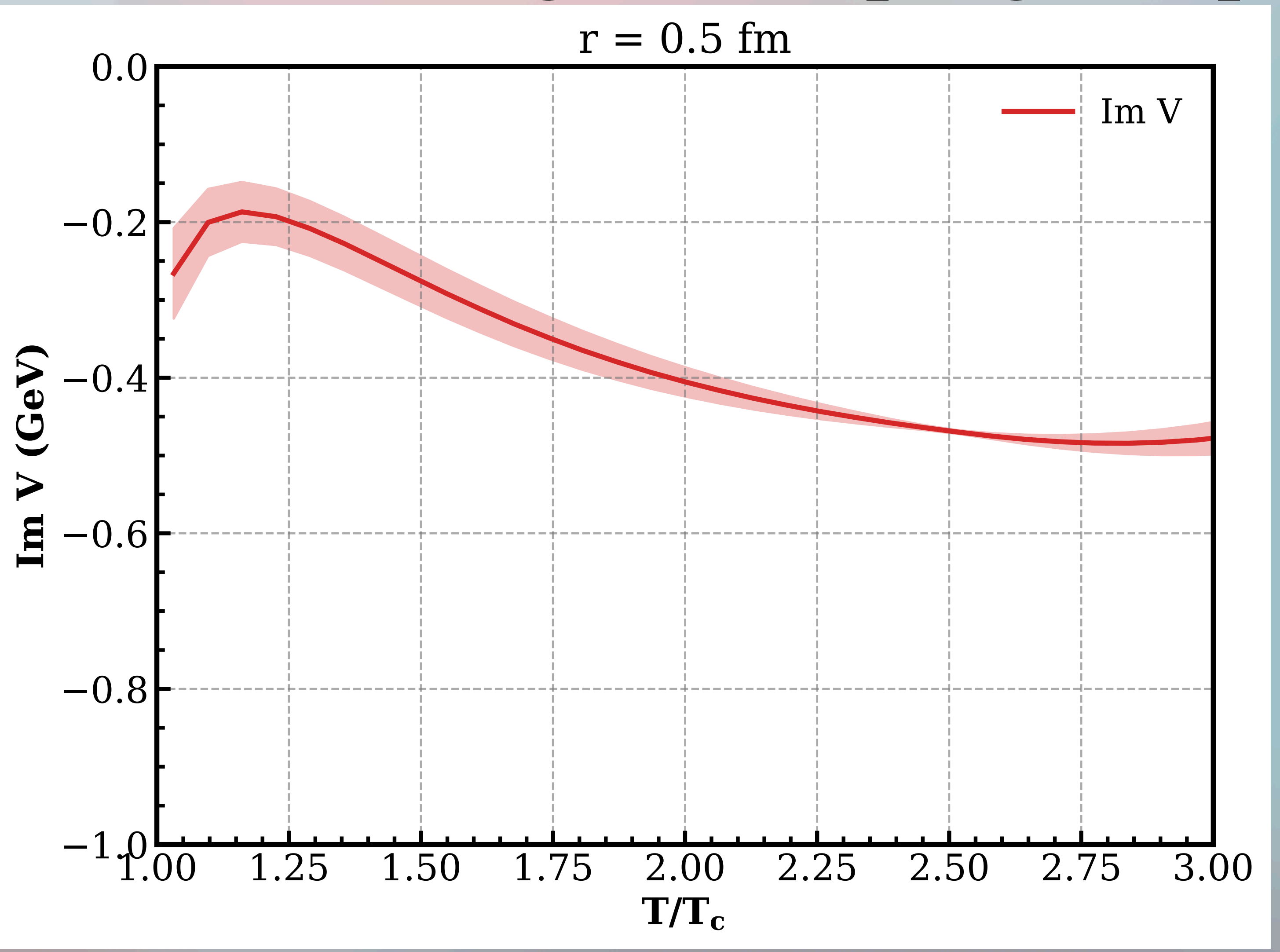

- M.Y.Jamal, F.P.Li, L.G.Pang and G.Y.Qin, [arXiv:2509.14970 [hep-ph]]

Dual Dissociation Criteria: $2E_B = \Gamma$ and $E_B = 3T$

- Width–binding crossover (upper bound): $2\,E_B(T) = \Gamma(T)\,.$

Interpretation: decoherence overtakes binding → rapid melting.

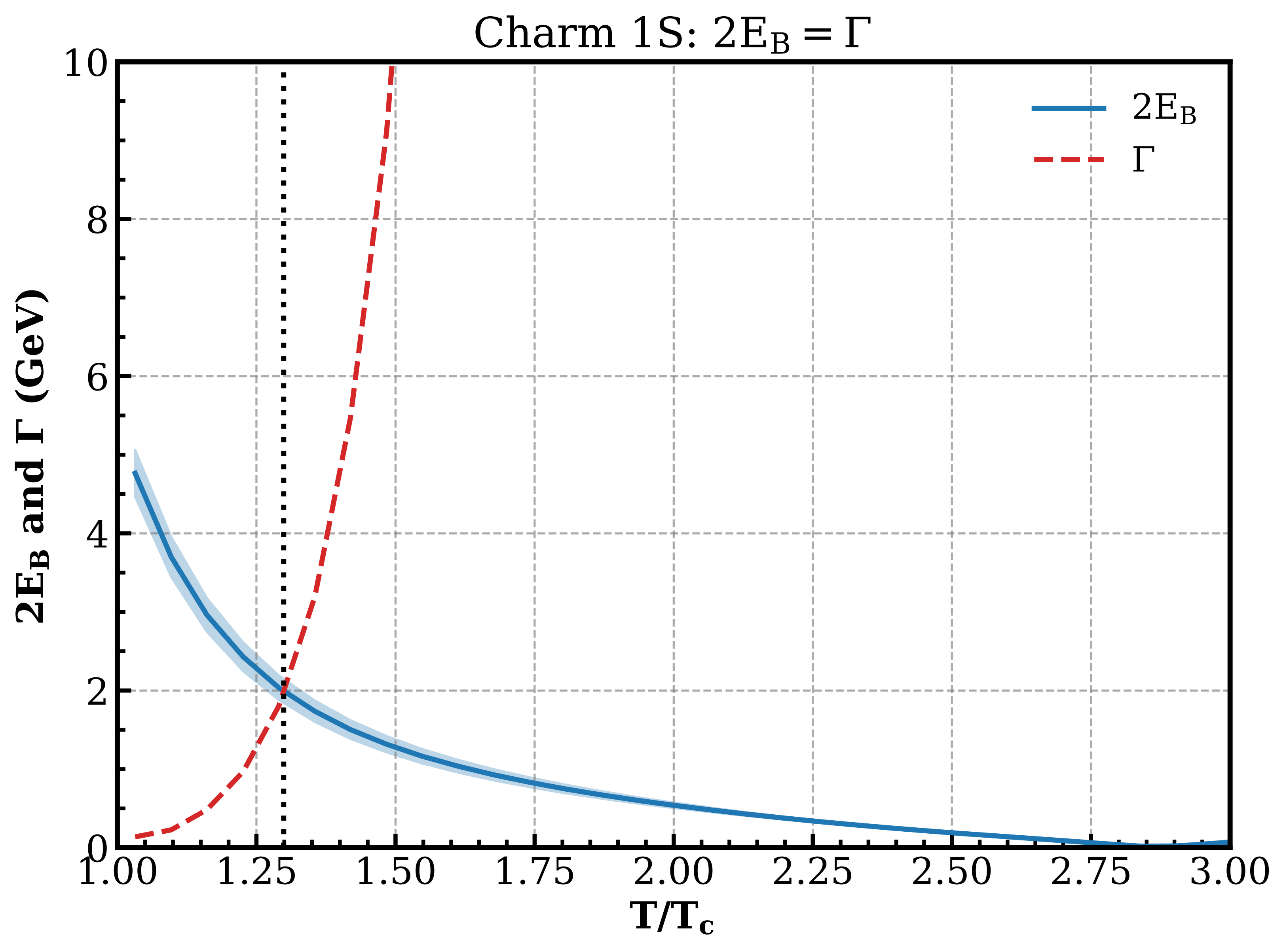

- Kinetic lower-bound (thermal smearing): $E_B(T) = 3\,T\,.$

Interpretation: binding comparable to typical thermal energy → weak survival.

- Y. Burnier and A. Rothkopf, PRL. 111, 182003 (2013).

Results—Charmonium and Bottomonium (Dissociation Temperatures)

$$T_d(\Upsilon(1S)) > T_d(J/\psi) \sim T_d(\Upsilon(2S)) > T_d(\psi(2S)),$$

- Hierarchy: $\Upsilon(1S)$ survives to the highest T; excited states melt earlier (sequential suppression).

Method / Reference	Dissociation Temperatures T_d (in units of T_c)			
	$\Upsilon(1S)$	$\Upsilon(2S)$	J/ψ	$\psi(2S)$
This work: $(2E_B = \Gamma)$	1.99	1.29	1.30	≤ 1.00
This work: $(E_B = 3T)$	1.38	1.10	1.13	≤ 1.00
Mocsy and Petreczky[1]	2.00	1.20	1.20	≤ 1.00
Digal et al.[2]	2.31	1.10	1.10	< 1.00

1: A. M'ocsy and P. Petreczky, PRL 99, 211602 (2007)

2: S. Digal, P. Petreczky, and H. Satz, PRD 64, 094015 (2001)

$$R_{AA}(\Upsilon(1S)) > R_{AA}(J/\psi) \sim R_{AA}(\Upsilon(2S)) > R_{AA}(\psi(2S)),$$

Future Directions

Future Possibilities

We are working the problems where ML can help in any possible way

- **Finite-Momentum Quarkonia**
  ML-based in-medium potentials to moving quarkonia including Doppler effects and anisotropic screening.

- **Phenomenology Connection: *Coupling to Realistic Medium Evolution***
  Use anisotropy-dependent widths in coupled transport+hydro evolution to predict ($R_{AA}(p_T)$) and (v_2).
  State-resolved inputs for LHC Run-3 and future EIC.

- **Magnetic Field and Chiral Effects**
  Study the combined impact of strong early-time magnetic fields on quarkonium binding and damping.

- **Pre-Equilibrium and Glasma Stage Dynamics**
  Incorporate quarkonium suppression mechanisms in the non-thermal early stages of heavy-ion collisions.

- **Beyond S-Waves: P-Wave States and Feed-Down Contributions**
  Achieve a complete, state-resolved description of quarkonium suppression patterns.

- **Bayesian/ML constrained potential uncertainty quantification**
  Tighten confidence bands on dissociation temperatures and rates.

Summary

- **Conceptual**

We built a unified pipeline from lattice QCD → medium properties → in-medium quarkonium observables.

- **Methodological**

Machine learning provides a smooth, uncertainty-controlled determination of quasiparticle masses and the Debye mass across the crossover region.

- **Physics Result**

The resulting complex potential naturally reproduces sequential quarkonium melting and yields dissociation temperatures consistent with phenomenological hierarchies.

- **Big-Picture Takeaway (Very Important)**

This framework bridges equilibrium lattice QCD and in-medium quarkonium physics, opening a path toward data-driven heavy-quarkonium tomography of the QGP.

Few works on Quarkonia

- ☑ **Medium-Induced Quarkonium Dissociation at Finite Chemical Potential and Weak Magnetic Field**
  Quarkonium stability in dense and magnetized QCD matter.

- ☑ **Quarkonia Mass Spectra and Thermodynamical Properties under Finite Magnetic Field**
  Magnetic field effects on quarkonium binding and spectra.

- ☑ **$c\bar{c}$ and $b\bar{b}$ Suppression in the Glasma**
  Quarkonium suppression in the pre-equilibrium glasma stage.

- ☑ **Quarkonia Dissociation at Finite Magnetic Field in the Presence of Momentum Anisotropy**
  Combined impact of magnetic field and anisotropic screening.

- ☑ **Impact of Medium Anisotropy on Quarkonium Dissociation and Regeneration**
  Directional medium effects on melting and recombination.

- ☑ **Liénard–Wiechert Potential of a Heavy Quarkonium Moving in QGP Medium**
  Electromagnetic analogy for moving quarkonium in plasma.

- ☑ **Dissociation of Heavy Quarkonia in Isotropic and Anisotropic Hot QCD Medium in a Quasiparticle Model**
  Quasiparticle model study of anisotropy-driven melting.

Thank you for your attention

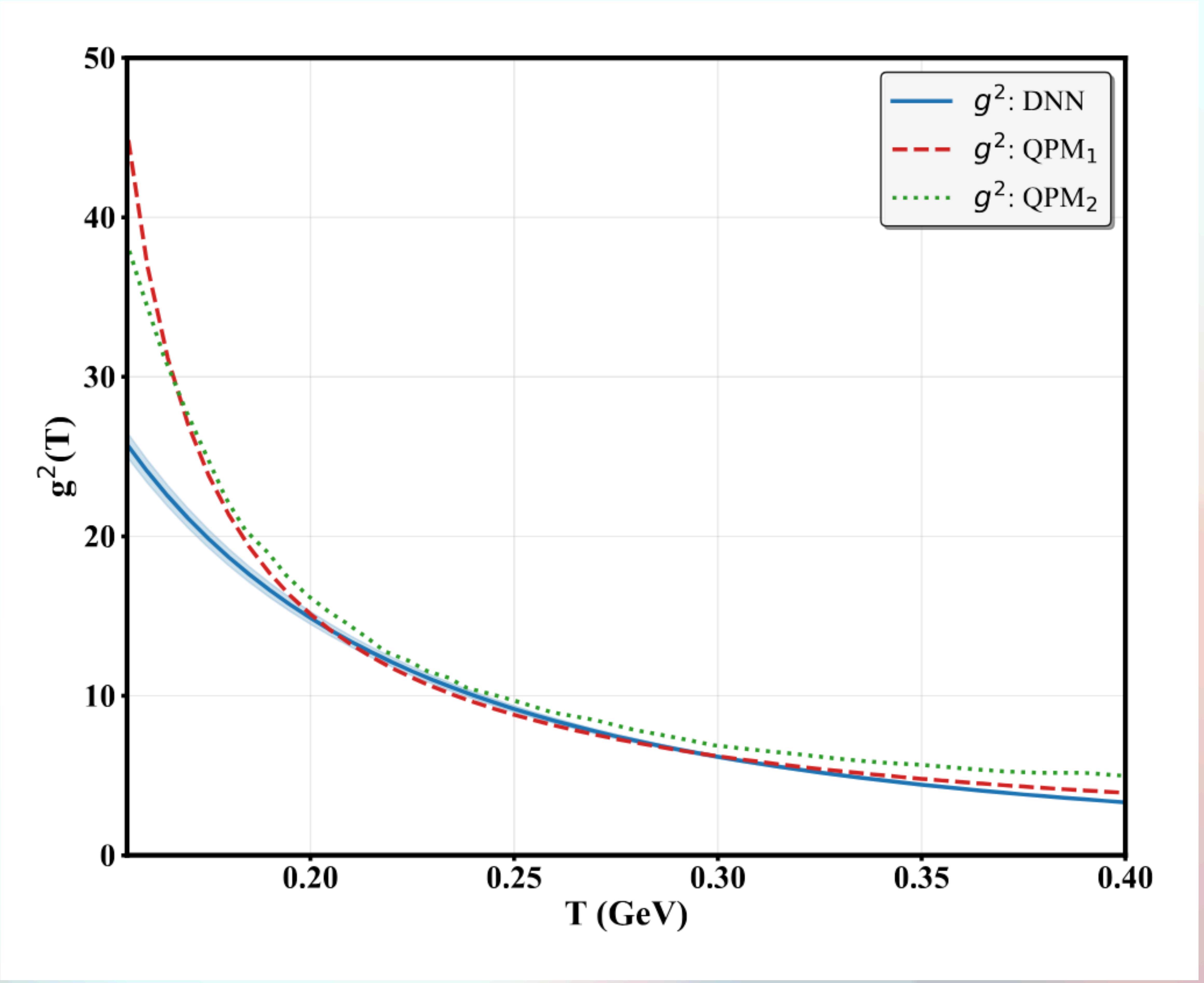

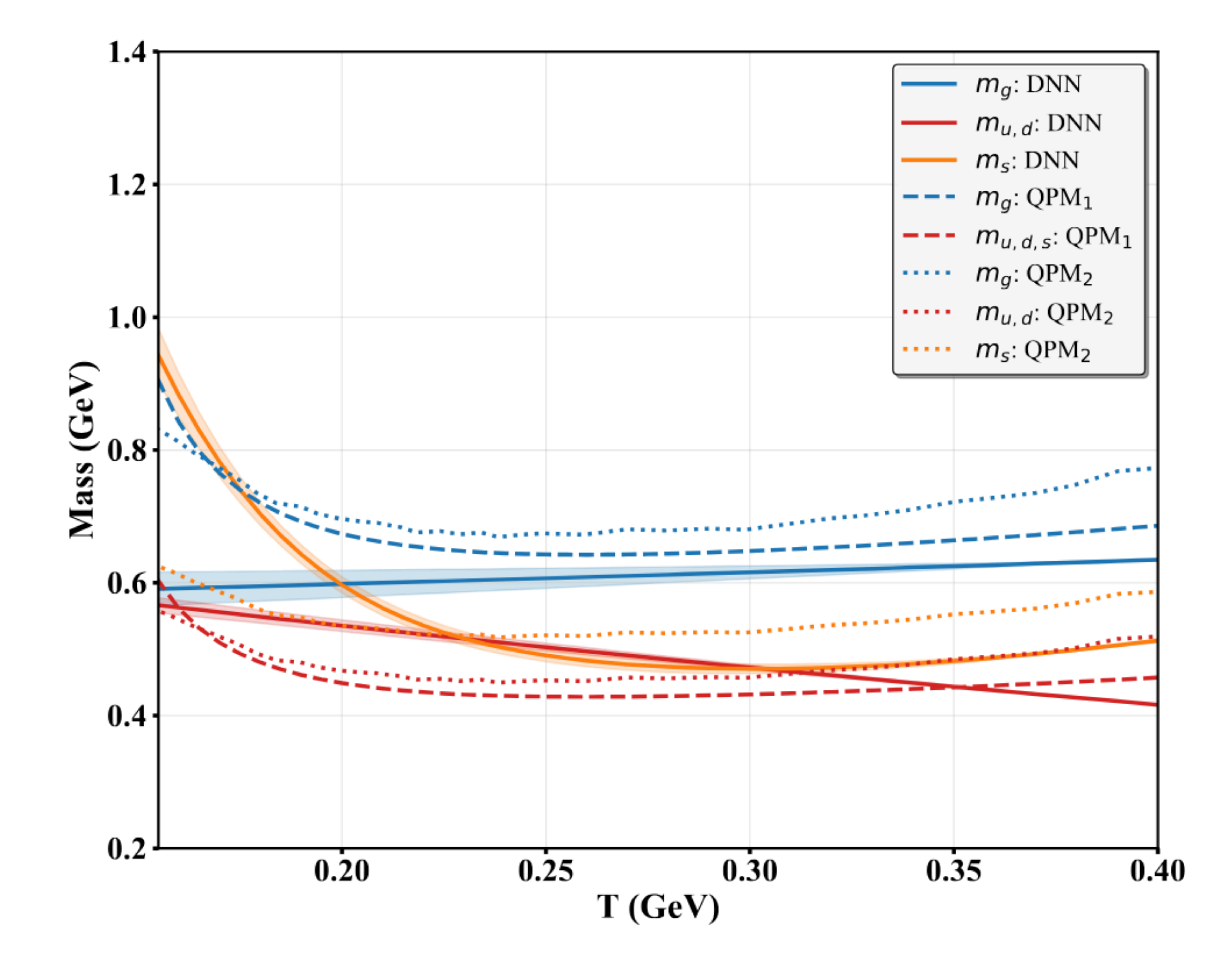

QPM 1: F.-L. Liu, W.-J. Xing, X.-Y. Wu, G.-Y. Qin, S. Cao,and X.-N. Wang, EPJC 82, 350 (2022)

QPM2: V. Mykhaylova, M. Bluhm, K. Redlich, and C. Sasaki, PRD 100, 034002 (2019)

• Result: $M(T)$ and η/s

$$\eta = \frac{1}{15T}\sum_i d_i \int \frac{d^3p}{(2\pi)^3}\tau_i \frac{p^4}{E_a^2} f_i(1 \mp f_i) \quad (1)$$

$$\tau_q^{-1} = 2\frac{N_C^2-1}{2N_C}\frac{g^2T}{8\pi}\ln\frac{2k}{g^2}, \tau_g^{-1} = 2N_C\frac{g^2T}{8\pi}\ln\frac{2k}{g^2} \quad (2)$$

$$g^2 = \frac{m_g^2 + m_{u/d}^2}{\left[\frac{1}{6}(N_C + \frac{1}{2}N_f) + \frac{N_C^2-1}{8N_C}\right]T^2} \quad (3)$$

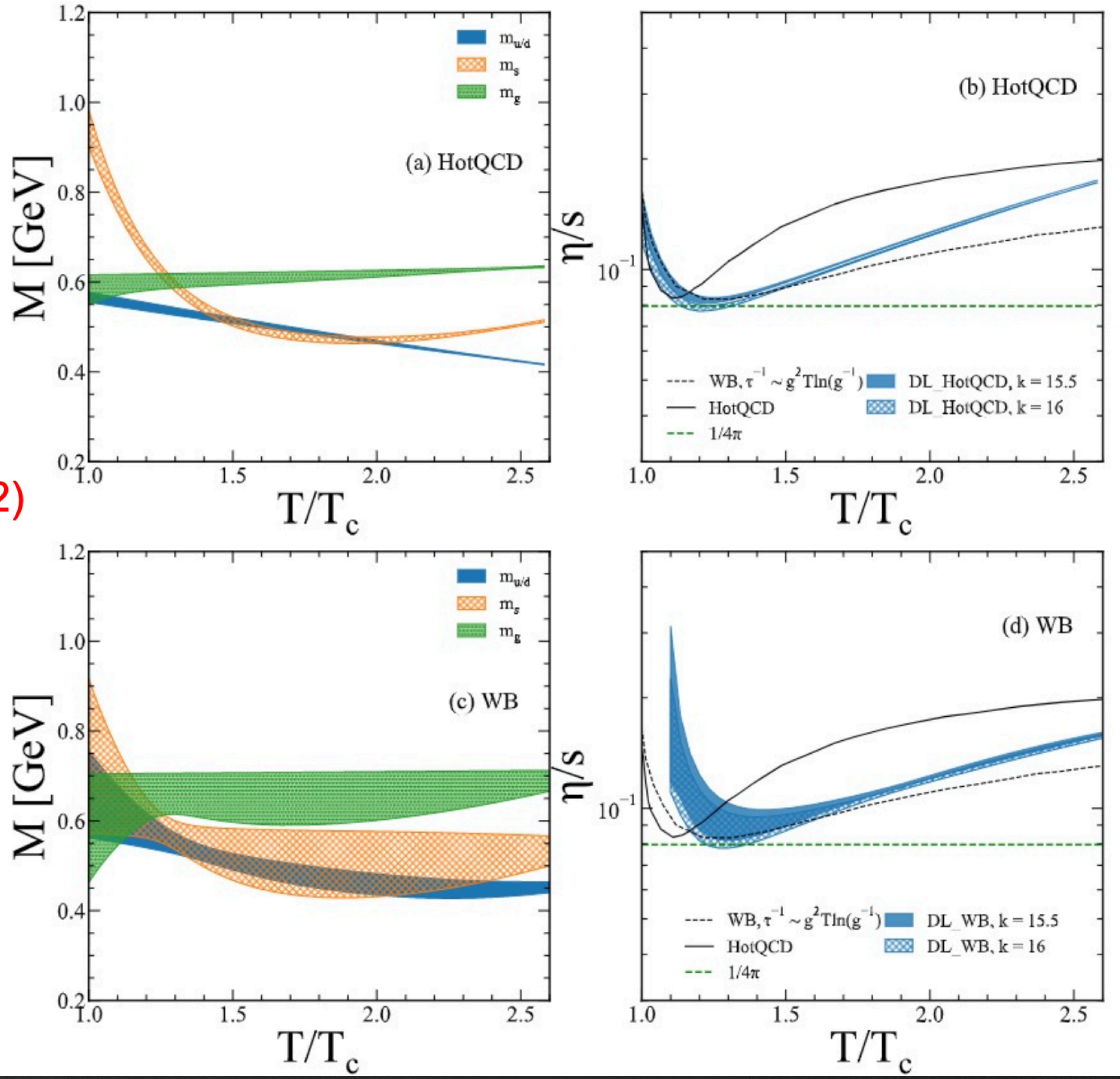

PHYSICAL REVIEW D 84, 094004 (2011)

F.P.Li, H.L.Lu, L.G.Pang and G.Y.Qin, PLB 844, 138088(2023)

Schrödinger Solver and Thermal Widths

- Radial bound states from

$$\left[-\frac{1}{2\mu}\frac{d^2}{dr^2}+\Re V(r,T)\right]u_n(r;T)=E_n(T)\,u_n(r;T),\quad \psi_n=u_n/r,\ \mu=\frac{m_Q}{2}\,.$$

- Binding energy with thermal continuum:

$$E_B(T)=V_\infty(T)-E_n(T)\,.$$

- Thermal width from Landau damping:

$$\Gamma_n(T)=4\pi\int_0^\infty dr\,r^2\,|\psi_n(r;T)|^2\left[-\,\Im V(r,T)\right].$$

- Numerics: dense r-grid (finite-difference); checked grid and $r_{\max}$ convergence.

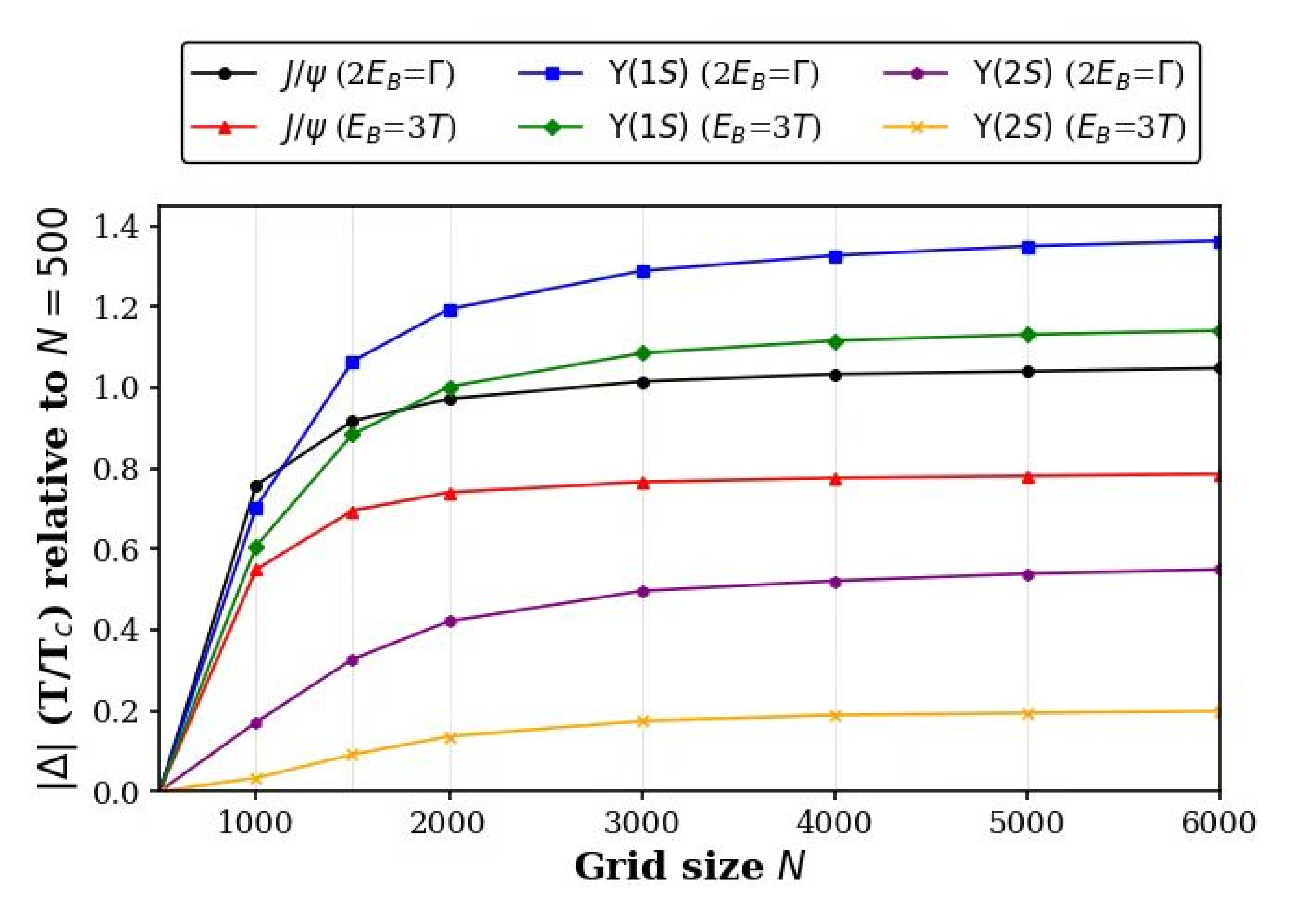

•M.Y.Jamal, F.P.Li, L.G.Pang and G.Y.Qin,[arXiv:2509.14970 [hep-ph]]

Loss Functions

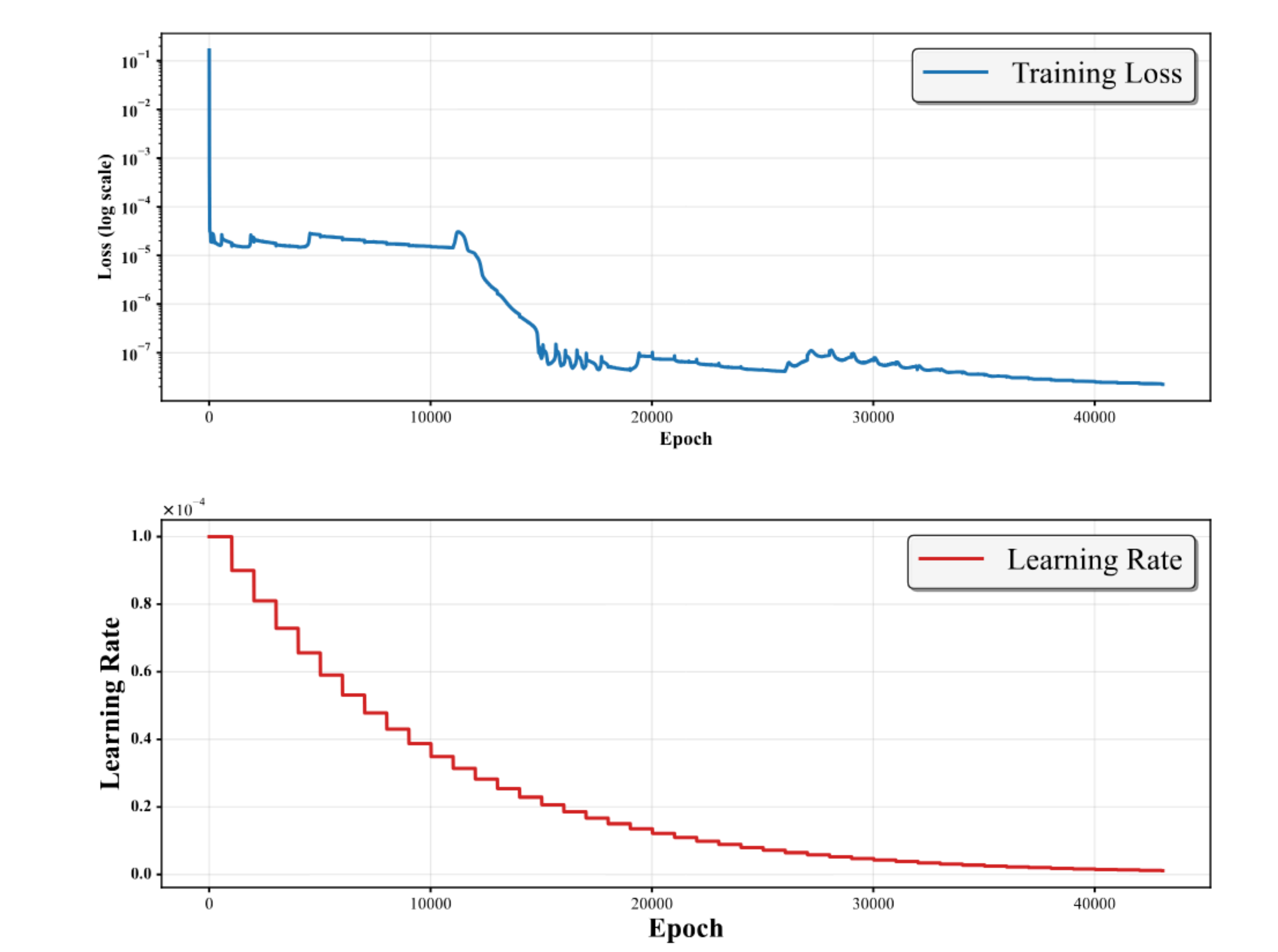

Dual Dissociation Criteria: $E_B = 3T$

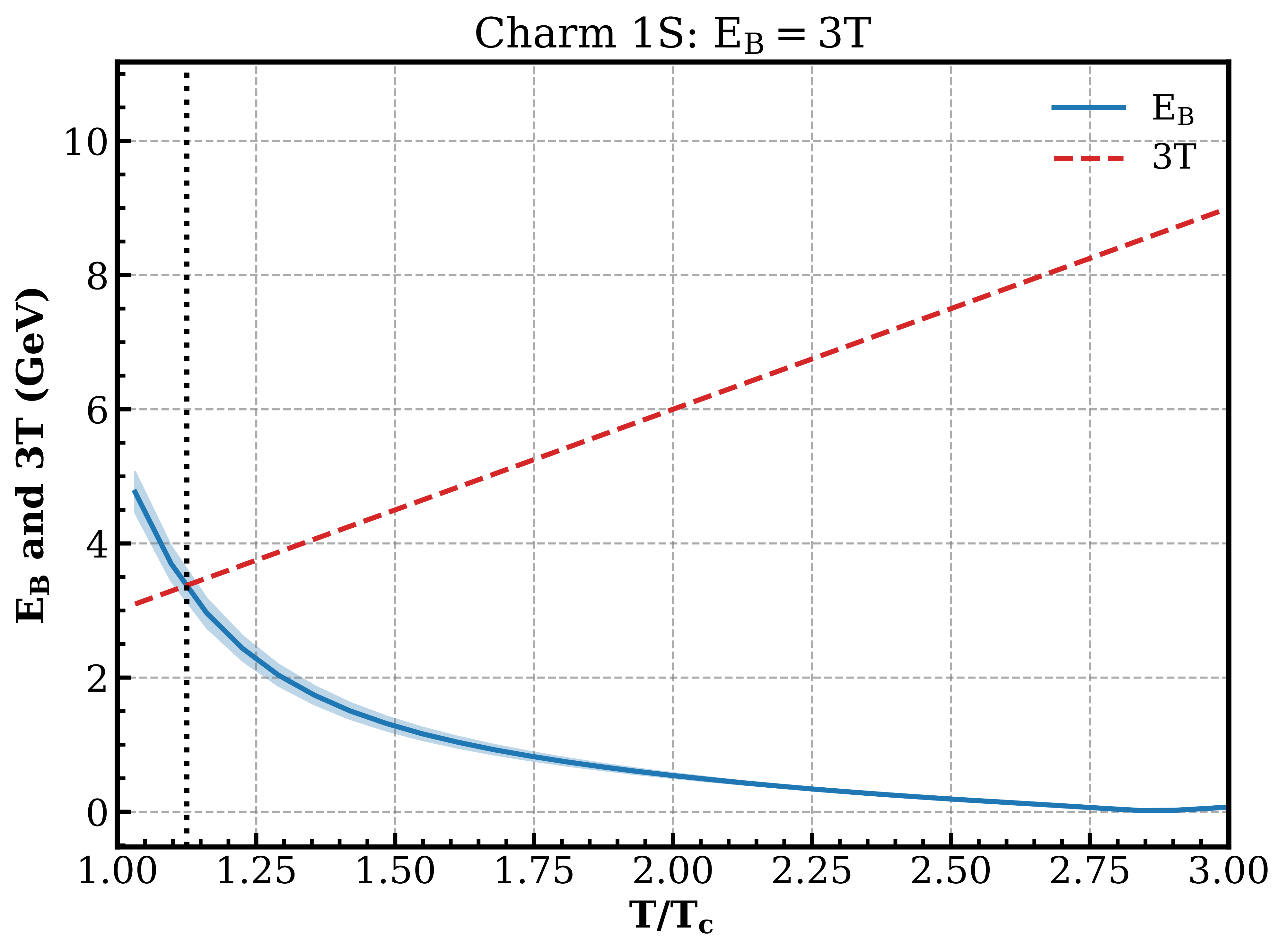

F.P.Li, H.L.Lu, L.G.Pang and G.Y.Qin, PLB 844, 138088(2023)

• Data: HotQCD

PHYSICAL REVIEW D **90**, 094503 (2014)

Equation of state in (2 + 1)-flavor QCD

A. Bazavov,[1] Tanmoy Bhattacharya,[2] C. DeTar,[3] H.-T. Ding,[4] Steven Gottlieb,[5] Rajan Gupta,[2] P. Hegde,[4] U. M. Heller,[6] F. Karsch,[7,8] E. Laermann,[8] L. Levkova,[3] Swagato Mukherjee,[7] P. Petreczky,[7] C. Schmidt,[8] C. Schroeder,[9] R. A. Soltz,[9] W. Soeldner,[10] R. Sugar,[11] M. Wagner,[5] and P. Vranas[9]
(HotQCD Collaboration)

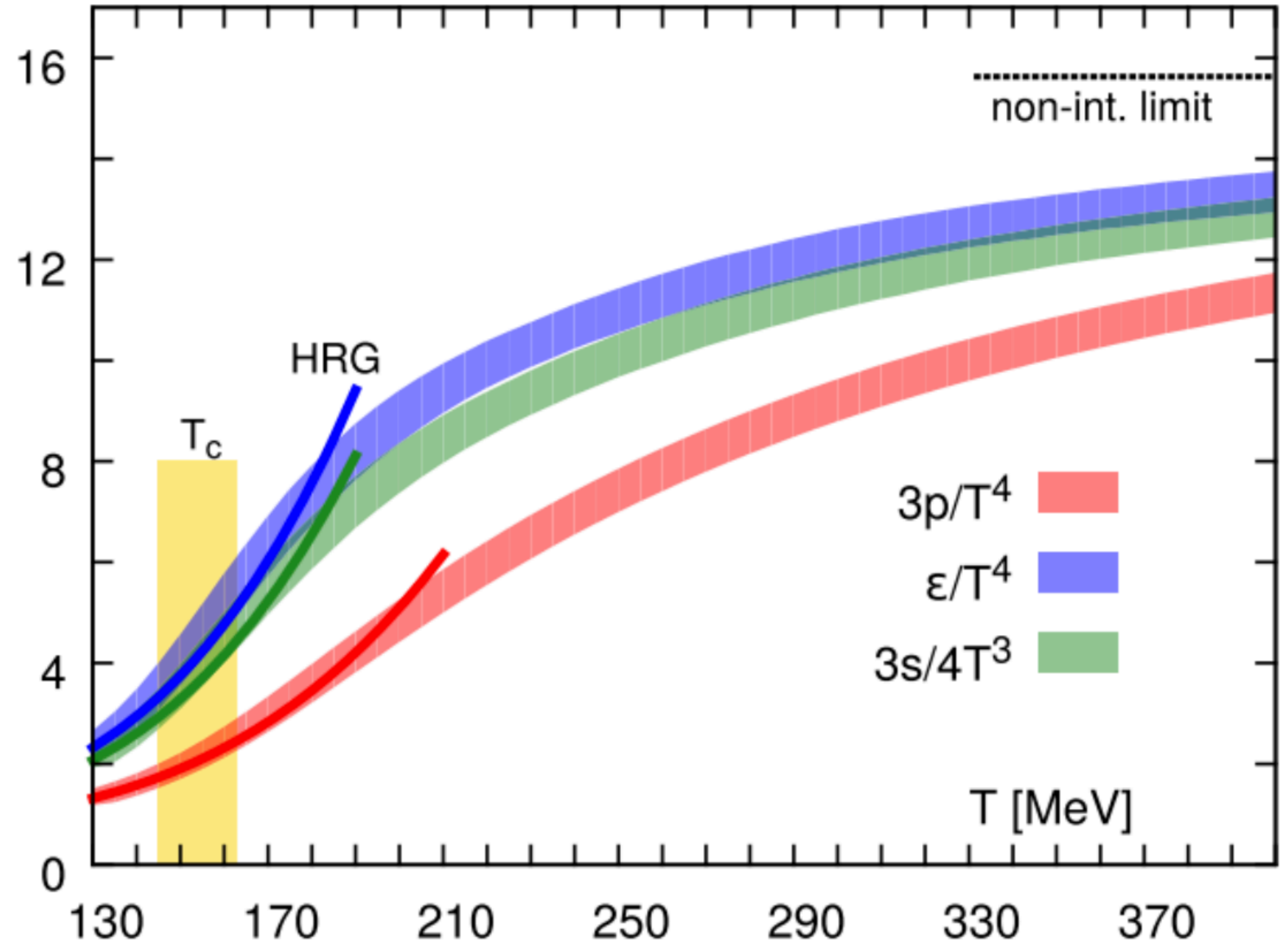

Physics Letters B 730 (2014) 99–104
Contents lists available at ScienceDirect
Physics Letters B
www.elsevier.com/locate/physletb
ELSEVIER

Full result for the QCD equation of state with 2 + 1 flavors

Szabolcs Borsányi [a], Zoltán Fodor [a,b,c], Christian Hoelbling [a], Sándor D. Katz [c,d,*], Stefan Krieg [a,b], Kálmán K. Szabó [a,e]

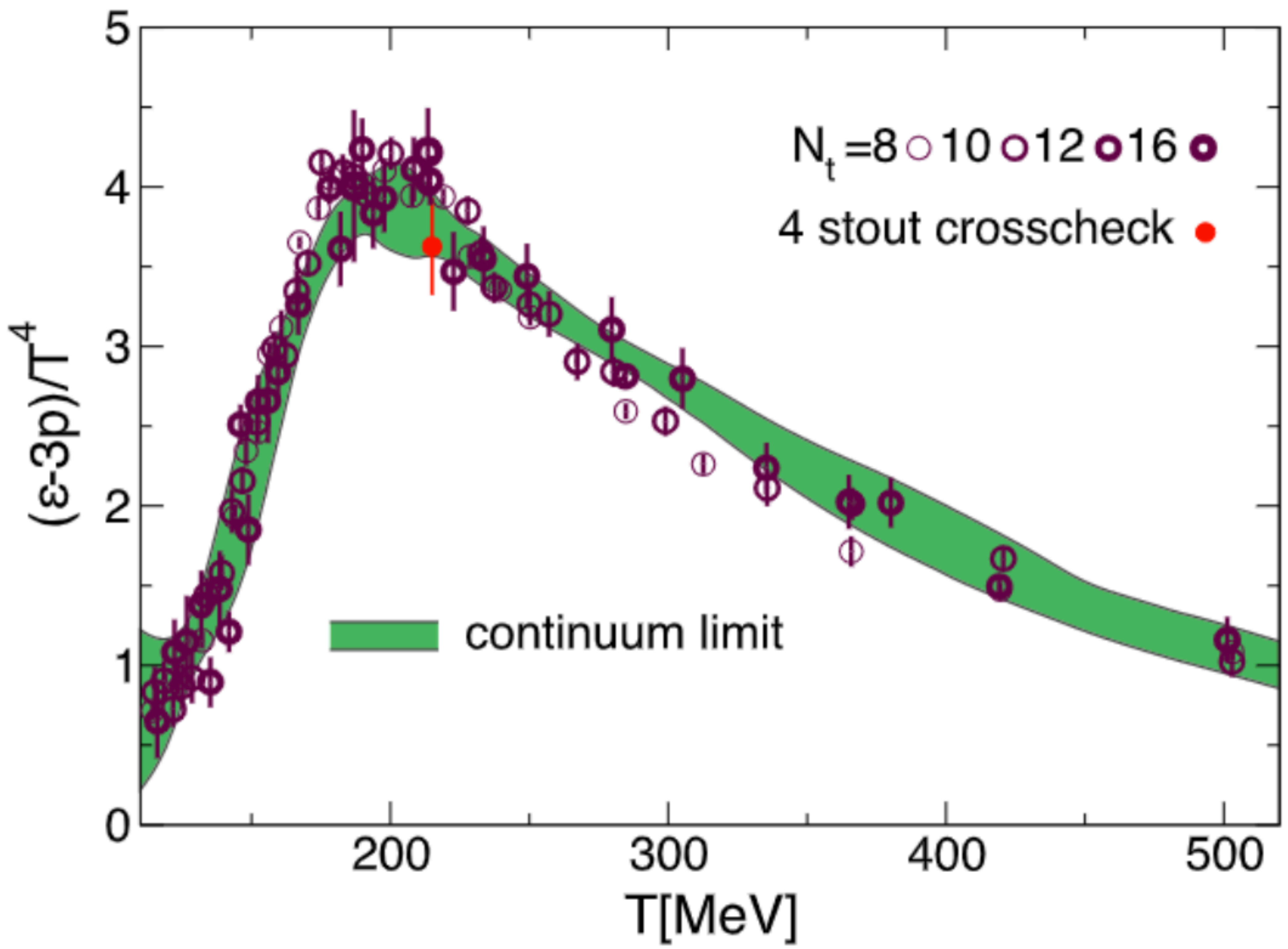

Method: Quasi particle method

$$\ln Z(T) = \ln Z_g(T) + \sum_i \ln Z_{q_i}(T)$$

$$\ln Z_g(T) = -\frac{d_g V}{2\pi^2} \int_0^\infty p^2 dp \ln\left[1 - \exp\left(-\frac{1}{T}\sqrt{p^2 + m_g^2(T)}\right)\right],$$

$$\ln Z_{q_i}(T) = +\frac{d_{q_i} V}{2\pi^2} \int_0^\infty p^2 dp \ln\left[1 + \exp\left(-\frac{1}{T}\sqrt{p^2 + m_{q_i}^2(T)}\right)\right],$$

$$P(T) = T\left(\frac{\partial \ln Z(T)}{\partial V}\right)_T$$

$$\epsilon(T) = \frac{T^2}{V}\left(\frac{\partial \ln Z(T)}{\partial T}\right)_V$$

d_g:the degree of freedom for gluons
d_{q_i}:the degree of freedom for quarks
q_i:up/down, strange quarks

F.P.Li, H.L.Lu, L.G.Pang and G.Y.Qin, PLB 844, 138088(2023)

DLQPM Details (Inputs, Network, Training)

- Inputs: lattice-QCD thermodynamics vs T: entropy $s(T)$ and interaction measure $\epsilon - 3p$ (HotQCD, continuum-extrapolated).
- Forward model: quasiparticle EOS with temperature-dependent masses $\{m_g(T), m_{u/d}(T), m_s(T)\}$; compute $p, s, \epsilon - 3p$ from these.
- Network: residual DNN mapping $T/T_c \to \{m_g, m_{u/d}, m_s\}$ with smoothness/monotonicity regularization and HTL-consistent high-T priors.
- Loss: MSE[$\mathrm{EOS}_{\mathrm{model}} - \mathrm{EOS}_{\mathrm{lattice}}$] + asymptotic penalties + regularizers; multiple random seeds → mean ± band.
- Output: calibrated $\{m_g, m_{u/d}, m_s\}$ with uncertainty; handed off to $\alpha_s(T)$ and $m_D(T)$ extraction.

Working Formulae (Potential, Widths):

- Vacuum Cornell:

$$V_{\text{vac}}(r) = -\frac{\alpha}{r} + \sigma r\,.$$

- Screened real part:

$$\Re V(r,T) \simeq -\alpha\,\frac{e^{-m_D r}}{r} + \frac{\sigma}{m_D}\left(1 - e^{-m_D r}\right), \quad V_\infty(T) = \frac{\sigma}{m_D} - \alpha\, m_D\,.$$

- Screened Imaginary Potential

$$\mathrm{Im}[V(r,T)] = \mathrm{Im}V_1(r,T) + \mathrm{Im}V_2(r,T),$$

$$\mathrm{Im}V_1(r,T) = -\,2\alpha T\int_0^\infty \frac{dz}{(z^2+1)^2}\left(1 - \frac{\sin(m_D r z)}{m_D r z}\right),$$

$$\mathrm{Im}V_2(r,T) = \frac{4\sigma T}{m_D^2}\int_0^\infty \frac{dz}{z(z^2+1)^2}\left(1 - \frac{\sin(m_D r z)}{m_D r z}\right).$$

- Observables:

$$E_B(T) = V_\infty(T) - E_n(T), \qquad \Gamma_n(T) = 4\pi\int_0^\infty dr\, r^2\,|\psi_n(r;T)|^2\,[-\,\Im V(r,T)]\,.$$

Numerics, Validation, and Sensitivity

- Schrödinger solver: finite-difference radial grid; Dirichlet at $r = 0$, $u_n(r_{\max}) \to 0$; check orthonormality and node counting for excited states.
- Convergence checks: scan grid size N and $r_{\max}$; monitor $\Delta E_n / E_n$ and stability of T_d from both criteria.

- Potential consistency: $\Re V(r \to 0, T)$ tracks vacuum limit; $V_\infty(T)$ monotone with $m_D(T)$.
- Uncertainty: propagate DLQPM retrain band $(\alpha_s(T), m_D(T))$ through E_B, Γ to T_d ranges.
- Sensitivity (typical): small variations in σ or short-distance α shift T_d modestly; dominant effect comes from $m_D(T)$ slope near T_c.

- Cross-checks: sequential hierarchy $\Upsilon(1S) > J/\psi \sim \Upsilon(2S) > \psi(2S)$ consistent with lattice spectral reconstructions and LHC R_{AA} ordering.